Hippo signaling pathway regulates cancer cell-intrinsic MHC-II expression

Zexian Zeng[1,2,3,4*], Shengqing Stan Gu[1,2,5,6,*], Nofal Ouardaoui[1], Carly Tymm[1], Lin Yang[1], Cheryl J Wong[1,7], Dian Li[1], Wubing Zhang[1,8], Xiaoqing Wang[5,6,1,2], Jason L Weirather[1,9], Scott J Rodig[9,10], F Stephen Hodi[5,9#], Myles Brown[5,6,#], X. Shirley Liu[1,2,6,#]

[*,#] indicate equal contributions

[1]Department of Data Science, Dana Farber Cancer Institute, Boston, MA, 02215, USA.
[2]Department of Biostatistics, Harvard T.H. Chan School of Public Health, Boston, MA, 02215, USA.
Current address: [3]Center for Quantitative Biology, Academy for Advanced Interdisciplinary Studies, Peking University, Beijing, 100084, China.
Current address: [4]Peking-Tsinghua Center for Life Sciences, Academy for Advanced Interdisciplinary Studies, Peking University, Beijing, 100084, China.
[5]Department of Medical Oncology, Dana-Farber Cancer Institute, Boston, MA, 02215, USA.
[6]Center for Functional Cancer Epigenetics, Dana-Farber Cancer Institute, Boston, MA, 02215, USA.
[7]Department of Biomedical Informatics, Harvard Medical School, Boston, MA 02115 USA.
[8]School of Life Science and Technology, Tongji University, Shanghai, 200060, China.
[9]Center for Immuno-Oncology, Dana-Farber Cancer Institute, Boston, MA, 02215, USA.
[10]Department of Pathology, Brigham and Women's Hospital, Boston, MA, 20115, USA.

Running Title:
Hippo regulates cancer-intrinsic MHC-II

Keywords:
MHC class II, immunotherapy response, Hippo signaling, gene regulation, melanoma

Financial support
This study was supported by the Breast Cancer Research Foundation [BCRF-20-100]; National Institutes of Health [R01CA234018, U24CA224316, T15LM007092]; Sara Elizabeth O'Brien Trust; and the Dana-Farber Cancer Institute. The funding bodies did not play any role in the design of the study and collection, analysis, and interpretation of data and in writing the manuscript. Publication costs are funded by Breast Cancer Research Foundation [BCRF-20-100].

Corresponding Authors
X. Shirley Liu, PhD
Professor, Department of Data Science
Dana-Farber Cancer Institute and Harvard University
Current address: 237 Putnam Ave, Cambridge, MA 02139, USA
Email: xsliu.res@gmail.com

Myles Brown, MD
Professor, Department of Medical Oncology
Dana-Farber Cancer Institute and Harvard Medical School
Address: 450 Brookline Ave, SM-1033, Boston, MA 02215, USA
Email: myles_brown@dfci.harvard.edu

F Stephen Hodi, MD
Professor, Department of Medical Oncology
Harvard Medical School and Dana-Farber Cancer Institute
Address: 450 Brookline Ave, DA-540, Boston, MA 02215, USA
Email: stephen_hodi@dfci.harvard.edu

Competing interests

S.J.R. has received research support from BMS, Merck, Affimed, and KITE/Gilead, and has been a member of the Science Advisory Boards for KITE/Gilead and Immunitas. M.B. is a consultant to and receives sponsored research support from Novartis. M.B. is a consultant to and serves on the scientific advisory boards of Kronos Bio, H3 Biomedicine, and GV20 Therapeutics. F.S.H. reports the following: grants from BMS and Novartis; personal fees from BMS, Merck, Serono, Novartis, Takeda, Surface Pharmaceuticals, Genentech/Roche, Compass Therapeutics, Apricity, Bayer, Aduro, Partners Therapeutics, Sanofi, Pfizer, Pionyr Immunotherapeutics, 7 Hills Pharma, Verastem Oncology, Rheos Medicines, and Kairos Therapeutics; equity in Torque Therapeutics; and patents #20100111973 and #7250291 issued as well as #20170248603, #20160340407, #20160046716, #20140004112, #20170022275, #20170008962, and “Methods of Using Pembrolizumab and Trebananib” pending. L. Sholl- honorarium from Astra Zeneca; consulting income from EMD Serono; research grant funding from Roche/Genentech. X.S.L conducted the work while being on the faculty at DFCI, and is currently a board member and CEO of GV20 Therapeutics. No potential conflicts of interest were disclosed by the other authors.

Words counts: 3,958
Number of figures: 6
Number of tables: 2

ABSTRACT

MHC-II is known to be mainly expressed on the surface of antigen-presenting cells. Evidence suggests MHC-II is also expressed by cancer cells and may be associated with better immunotherapy responses. However, the role and regulation of MHC-II in cancer cells remain unclear. In this study, we leveraged data mining and experimental validation to elucidate the regulation of MHC-II in cancer cells and its role in modulating the response to immunotherapy. We collated an extensive collection of omics data to examine cancer cell-intrinsic MHC-II expression and its association with immunotherapy outcomes. We then tested the functional relevance of cancer cell-intrinsic MHC-II expression using a syngeneic transplantation model. Lastly, we performed data mining to identify pathways potentially involved in the regulation of MHC-II expression, and experimentally validated candidate regulators. Analyses of pre-immunotherapy clinical samples in the CheckMate 064 trial revealed that cancer cell-intrinsic MHC-II protein was positively correlated with more favorable immunotherapy outcomes. Comprehensive meta-analyses of multiomics data from an exhaustive collection of data revealed that MHC-II is heterogeneously expressed in various solid tumors, and its expression is particularly high in melanoma. Using a syngeneic transplantation model, we further established that melanoma cells with high MHC-II responded better to anti–PD-1 treatment. Data mining followed by experimental validation revealed the Hippo signaling pathway as a potential regulator of melanoma MHC-II expression. In summary, we identified the Hippo signaling pathway as a novel regulator of cancer cell-intrinsic MHC-II expression. These findings suggest modulation of MHC-II in melanoma could potentially improve immunotherapy response.

Synopsis

High cancer-intrinsic expression of MHC-II is associated with better immunotherapy responses and clinical outcomes. Multiomic analyses and gene editing experiments demonstrate that MHC-II expression is regulated by the Hippo signaling pathway in melanoma.

Introduction

The major histocompatibility complex class II (MHC-II) molecule is essential for stimulating CD4+ T cell–dependent immune responses (1). It is highly expressed on the surface of professional antigen-presenting cells (APCs) such as dendritic cells, B cells, macrophages, and thymic epithelial cells (2,3). By loading endosome/lysosome-processed antigenic peptides on MHC-II, APCs can interact with antigen-specific CD4+ T cells and induce their activation/differentiation (2-4). Evidence has revealed that cancer cells can also express MHC-II, especially when stimulated by inflammatory cytokines such as IFNγ (5,6). In addition, cancer cell-intrinsic MHC-II expression is reported to be associated with better responses to immune checkpoint blockade (ICB) treatment in patients with melanoma or classic Hodgkin lymphoma (7-9). Furthermore, the presence of intratumoral cytotoxic CD4+ T cells in patients with metastatic bladder cancer was positively correlated with anti–PD-L1 response (4). Together, these studies implicate cancer cell-intrinsic MHC-II as a potential modulator of antitumor immunity and immunotherapy response. However, it is unclear whether cancer cell-intrinsic MHC-II results in more favorable immunotherapy outcomes.

The class II transactivator (*CIITA*) transcription factor is known as a major regulator of MHC-II gene expression (3,5,10). Several studies ectopically overexpressed CIITA in mouse cancer cells, which led to increased cancer cell-intrinsic MHC-II expression and elevated sensitivity to anti–PD-1 treatment (11,12). However, ectopic overexpression of CIITA might exceed biologically relevant quantities. It remains unclear whether the natural variation in cancer cell-

intrinsic MHC-II expression leads to differential anti-tumor immune response. Furthermore, although *CIITA* is an important regulator of MHC-II expression, other factors affecting cancer cell-intrinsic MHC-II expression remain to be determined (13,14).

To better understand the role and regulation of MHC-II in cancer cells, we herein thoroughly profiled and analyzed MHC-II expression using multiomics data derived from large collections of cancer cells and patient samples. Our analyses revealed a positive correlation between cancer cell-intrinsic MHC-II protein abundance and immunotherapy outcomes in patients with melanoma. Examination of human cancer cell lines showed that MHC-II is highly expressed in skin cancer cells compared to other solid tumor types. To elucidate the role of cancer cell-intrinsic MHC-II in modulating immunotherapy response, we evaluated *in vivo* the anti–PD-1 response of isogenic melanoma cells with high or low MHC-II expression. Our results showed that MHC-II-high melanoma cells exhibited a more favorable anti–PD-1 response. Furthermore, data mining followed by experimental validation revealed the Hippo signaling pathway as a regulator of MHC-II in melanoma. Our study implicates the important role of MHC-II in the immunotherapy response and suggests the Hippo signaling pathway as a potential means of modulating its expression.

Materials and Methods

Data curation

To examine cancer cell-intrinsic MHC-II expression and its regulation, we collated an extensive collection of omics data from data consortia and published studies (**Table 1**). For pan-cancer human cancer cell lines, we only included cohorts with sample sizes larger than 500. For melanoma datasets, we included cohorts with sample sizes larger than 50 or cohorts that have multiplex omics data profiled. Specifically, we collected and curated human cancer cell line data from DepMap (15), comprising 1362 RNA-Seq and 367 mass spectrometry profiles (16). RNA-

Seq profiles of 675 human cancer cell lines were collected from the Klijina study (E-MTAB-2706) (17) and 54 melanoma cell lines from the Tsoi study (GSE80829) (18). Proteomic and phosphoproteomic data of six melanoma cancer cell lines were collected from the Gao study (GSE162270) (19). We also integrated orthogonal proteomic and epigenomic data of melanoma cell lines to examine potential regulators of cancer cell-intrinsic MHC-II. Specifically, we collected transcriptome and chromatin accessibility data from the Verfaillie study (GSE60666) (20), where RNA-Seq and FAIRE-Seq were profiled for ten melanoma cell lines. The Verfaillie study (GSE60666) (20) also provided RNA-Seq profiles of three melanoma cell lines with TEADs (*TEAD1*, *TEAD2*, *TEAD3*, *TEAD4*) knockdown (KD) and their matched controls. Specifically, siRNA-mediated gene knockdown experiments were performed for the TEADs KD (20). Furthermore, to examine cancer cell-intrinsic MHC-II's role in clinical samples, we utilized data from CheckMate 064, a randomized phase 2 study (NCT01783938) evaluating the sequential combination of nivolumab followed by ipilimumab, or the reverse sequence of ipilimumab followed by nivolumab, in patients with histologically confirmed unresectable stage III or stage IV melanoma (21). In additional to RNA-Seq data, immunohistochemistry (IHC) was also used to quantify the percent of cancer cells expressing MHC-II using the markers of *HLA-DP*, *HLA-DQ*, *HLA-DR*, and *SOX10* (8). Moreover, we collected human melanoma single-cell RNA-Seq (scRNA-Seq) (22) dataset to evaluate the correlation between cancer cell-intrinsic MHC-II expression and T-cell infiltration.

Cell lines and cloning of sgRNAs for CRISPR validation

Cell lines A375 (human melanoma) and B16F10 (mouse melanoma) were purchased from the American Type Culture Collection (ATCC) and authenticated using standard short tandem repeat analysis in 2019. Both cell lines were cultured in Dulbecco's Modified Eagle Medium (DMEM, Corning #10013CV) supplemented with 10% fetal bovine serum (FBS, Sigma-Aldrich

#F2442), 1% L-glutamine (Life Technologies #25030164), and 1% penicillin and streptomycin (Life Technologies #15140163). Both cell lines were routinely screened for Mycoplasma infection using the MycoAlert Mycoplasma Detection Kit (Lonza), and used within four passages in culture after thawing.

We cloned four gRNAs targeting each of the genes: *CIITA*, *NF2*, *AMOTL1*, *AMOTL2*, *LATS1*, *LATS2*, *RUNX1*, and *CBFB* into the LentiCRISPRv2-Puro construct following a previously established protocol (23). Briefly, gRNAs for each gene were individually cloned into the lentiCRISPRv2-Puro vector purchased from Addgene (Plasmid #52961). DNA oligos for gRNA cloning were purchased from Invitrogen. The sequences of gRNAs are listed in Table 2.We produced lentivirues by lipofectamine 3000 transfection reagent (Invitrogen #L3000015) and transduced A375 cells in the presence of 8ug/ml polybrene (Millipore #TR10003G).

Flow cytometry

We performed fluorescence-activated cell sorting (FACS) of A375 cells treated under the indicated conditions to quantify HLA-DR. A375 cells were dissociated by enzyme-free Hanks dissociation buffer (Life Technologies # 13150016), washed with Phosphate-buffered saline (PBS, Corning # MT21040CV)-2%FBS, and incubated with DAPI (1:10,000 dilution, Life Technologies) and anti-HLA-DR (clone L243, BioLegend, 1:200 dilution) for 1 hour on ice. Cells were then washed and resuspended in PBS-2%FBS and analyzed on the BD LSR-Fortessa instrument. FACS data were analyzed by FlowJo. For separation of MHC-II-high and -low B16F10 cells, we first treated the cells with 10ng/ml IFNγ (Peprotech #315-05) for 48 hours, and FACS-sorted the cells into MHC-II-high and -low subpopulations based on their I-A/I-E (mouse MHC-II) expression (by anti-mouse I-A/I-E, clone M5/114.15.2, BioLegend). The cells that showed higher MHC-II than the untreated B16F10 population were sorted as MHC-II-high cells, whereas the cells that showed comparable MHC-II with untreated B16F10 were sorted as MHC-

II-low cells. The MHC-I abundance of B16F10 cells was measured by flow cytometry using anti-mouse H2-Kb (clone AF6-88.5, BioLegend).

Mice

All mice were housed in standard cages in the Dana-Farber Cancer Institute Animal Resources Facility (ARF). All animal procedures were carried out in accordance with the ARF Institutional Animal Care and Use Committee (IACUC) protocol and with the approval of IACUC. All murine experiments were performed in compliance with institutional guidelines as approved by the IACUC of Dana-Farber Cancer Institute. Mice were euthanized using CO_2 inhalation. Wild-type C57BL/6 recipient mice were purchased from Charles River Laboratories.

We transplanted $4x10^5$ MHC-II-high or -low B16F10 cells per site subcutaneously into the left and right flanks of 6-8 week-old male C57BL/6 mice (2 sites/mouse, 10 mice/group). From day 3 post-transplantation, we treated mice intraperitoneally with control IgG (clone 2A3, BioXCell, 100μg per mouse) or anti–PD-1 (clone 1A12, BioXCell, 100μg per mouse) every 3rd day for a total of 4 treatments. We monitored tumor growth, and the maximum tumor diameter permitted of 20mm was not exceeded.

Data processing and statistical analyses

For each sample, the transcriptomic profile was $\log_2(1+TPM)$ transformed. Pearson's correlation was performed to investigate associations between MHC-II expression and biomarkers and pathways. Adjusted p-values were retrieved and reported for each biomarker and pathway. To make reliable and robust immune cell infiltration estimations, we utilized Immunedeconv (24), an R package that integrates state-of-the-art algorithms for immune deconvolution, including TIMER (25), xCell (26), CIBERSORT (27), EPIC (28), quanTIseq (29), and MCPcounter (30). Although each algorithm has unique properties and strengths (24), immune infiltration

estimations supported by multiple algorithms provide more confident results. To make reliable immune infiltration estimations, we used six state-of-the-art algorithms, hoping to identify immune cell types consistently inferred by various algorithms.

Differentially expressed or top-ranked genes were selected for pathway enrichment studies. The pathway enrichment for each sample was evaluated by single sample gene set enrichment analysis (ssGSEA) (31). The MHC-I signature is comprised of *HLA-A*, *HLA-B*, *HLA-C*, and *B2M* genes, and the MHC-II signature contains *CIITA, CD74, HLA-DMA, HLA-DMB, HLA-DOA, HLA-DOB, HLA-DPA, HLA-DPB, HLA-DQA, HLA-DQB, HLA-DRA,* and *HLA-DRB* genes. To identify genes/pathways correlated with cancer-intrinsic MHC-II expression, we used 10 melanoma cell lines that have matched transcriptomic and epigenomic data; 6 melanoma cell lines that have matched proteomics and phosphoproteomics data; 33 melanoma cell lines that have matched proteomics and transcriptomic data (Table 1). In each data cohort, we first evaluated proteomic or transcriptomic MHC-II abundance for each sample using ssGSEA (31). With MHC-II expression derived, we further used Pearson correlation to calculate each phosphopeptide's association with the MHC-II expression. For these analyses, we examined their top enriched pathways and focused on the ones that were consistently enriched across different analyses. To identify gene expression programs associated with MHC-II expression, we curated three independent melanoma cell line cohorts that were profiled by RNA-seq (n=83; n=54; n=53;) (Table 1). In each melanoma cell line cohort, we also calculated each gene's Pearson correlation with the calculated MHC-II expression. Genes significantly (FDR<0.05) correlated with MHC-II expression were selected for pathway enrichment studies. For these three analyses, we examined their top genes/pathways and particularly focused on the ones that were significant in all cohorts.

Statistical analyses were performed using R3.6 and GraphPad Prism8. The growth of primary tumors was analyzed using two-way ANOVA with multiple comparisons. When analyzing scRNA-seq data, we used pseudobulk method as it was reported to produce fewer false positives compared to other single-cell methods (32). Unpaired Student's t-test, or unpaired two-sided Mann–Whitney test were used as indicated for comparisons between two groups. Kaplan–Meier overall survival curves were used to estimate survival in different comparison groups. Cox proportional hazards regression analysis was used to test the significance of the associations. All p-values are two-sided, and statistical significance was evaluated at 0.05. Corrections for multiple testing were performed with the false discovery rate (FDR).

Data availability

CCLE data is available at the https://depmap.org/portal/ccle/ data portal. CheckMate 064 (NCT01783938) is available through a direct application from Bristol Myers Squibb (BMS). All other data are publicly available at Array Express or Gene Expression Omnibus (GEO) with accession codes of E-MTAB-2706, GSE80829, GSE162270, GSE60666, and GSE72056.

Results

High cancer cell-intrinsic MHC-II is associated with favorable immunotherapy outcomes

It was reported that cancer cell-intrinsic MHC-II expression is positively correlated with immunotherapy response (7,8). Inspired by these studies, we asked what underlies this correlation by examining the immune infiltration of MHC-II-high and MHC-II-low tumors. Specifically, we curated CheckMate 064 (21), a clinical trial of nivolumab given sequentially with ipilimumab (regimen switched in week 13) in subjects with advanced or metastatic melanoma. Biopsies in CheckMate 064 were collected prior to immunotherapy, and both cancer cell-intrinsic MHC-I and MHC-II protein abundances were quantified by IHC (8). Consistent with the original publication (8), we found that high MHC-II protein in pre-immunotherapy samples was

associated with better patient immunotherapy response, 25-week progression free survival (PFS), and overall survival (OS) (**Fig. 1A-B**).

To further examine the correlations between cancer cell-intrinsic MHC protein and immune infiltration, we computationally inferred the tumor immune infiltration using expression profiles measured on the bulk tumors. Tumor immune infiltration was inferred using six state-of-the-art immune deconvolution algorithms for robust results (**Materials and Methods**). We further correlated the cancer cell-intrinsic MHC-I/II expression with inferred immune infiltration. In accordance with previous studies, cancer cell-intrinsic MHC-I protein was highly associated with CD8+ T-cell infiltration (**Fig. 1C**) (**Supplementary Table S1**). We also found that cancer cell-intrinsic MHC-II protein was positively correlated with CD8+ T cell, CD4+ T cell, and B-cell infiltration (**Fig. 1D**) (**Supplementary Table S2**). Notably, this correlation between the inferred T-cell infiltrates and the MHC-II protein is even stronger within the ICB responders (**Fig. S1A**, **Supplementary Table S3-S4**), raising the possibility that it might be associated with a pro-inflammatory anti-tumor response. To further test our hypothesis, we curated a single-cell RNA-seq dataset (22), which profiled not only immune cells, but also 4,645 cancer cells from 19 melanoma patient tumors. Using this dataset, we confirmed that the MHC-II expression of cancer cells is significantly correlated with number of T cells in the sample (**Fig. S1B**). We next examined whether MHC-II protein was correlated with MHC-I protein. From the CheckMate 064 study, where MHC-I and MHC-II proteins were profiled by IHC, we did not observe a significant correlation between these two MHC complexes (Pearson correlation p=0.25) (**Fig. S1C**). This suggests that MHC-II expression is not simply a natural consequence of MHC-I expression.

MHC-II is highly expressed in skin cancer cells and associated with immunotherapy response

We next wondered whether the expression of cancer cell-intrinsic MHC-II is a common phenomenon across cancer types. Due to the lack of quantified cancer cell-intrinsic gene expression in published clinical cohorts, we examined the MHC-II expression in cancer cell lines using data from multiple data consortia and published studies (**Table 1**). Leveraging these curated data, we first investigated the roles and patterns of cancer cell-intrinsic MHC-II. We performed transcriptome analyses on human cancer cell lines from the Cancer Cell Line Encyclopedia (CCLE) (15) and observed variable MHC-II expression across cancer types. Specifically, MHC-II is highly expressed in hematologic cancers, including leukemia, lymphoma, and myeloma (**Fig. 2A**). In addition, MHC-II is also expressed in multiple solid tumor cancer types, among which skin cancer has the highest expression (**Fig. 2A**). The high expression of MHC-II in skin cancer cells was also confirmed in the Klijina study (17), an independent cohort with 675 profiled cell lines (**Fig. 2B**). To further examine whether these observations were consistent with protein abundance, we curated 367 cell lines from the CCLE, where protein expression was measured by mass spectrometry. Using this dataset, we consistently observed a high MHC-II protein expression in the skin cancer cell lines (**Fig. S1D)**, which was correlated with high MHC-II gene transcription (p=6.2e-13) (**Fig. 2C**). The high correlation between MHC-II mRNA and protein was observed in most cancer types (**Fig. S1E**). Together, analyses of the transcriptomic and proteomic data suggest that the MHC-II is heterogeneously expressed in solid tumor cancer cells, with the highest expression in skin cancer.

Based on these analyses, we asked whether cancer cell-intrinsic MHC-II expression influences ICB response, or is merely a biomarker for intratumoral immune infiltration. B16F10 is a widely used syngeneic melanoma model for testing cancer immunotherapy. It can be induced to express MHC-II by treatment with IFNγ, showing good potential to examine the effects of MHC-II on immunotherapy response. We first sorted B16F10 cells into MHC-II-high and -low subpopulations based on their IFNγ-induced MHC-II expression. We noted that the MHC-II-high

cells showed higher MHC-II but similar MHC-I compared to MHC-II-low cells (**Fig. S2**). We then expanded the sorted cells and tested their response to anti–PD-1 *in vivo* (**Fig. 3A**). MHC-II-high cells showed a significant response to anti–PD-1, whereas MHC-II-low cells showed no response (**Fig. 3B**). These results suggest that in this model, anti–PD-1 response mainly comes from the MHC-II-high cells. Previous studies tested the effects of cancer cell-intrinsic MHC-II by ectopically expressing CIITA (11,12), even beyond biologically relevant quantities. In contrast, our study addressed this question by separating isogenic cells according to natural variation in MHC-II abundance, confirming the relationship between cancer cell-intrinsic MHC-II and immunotherapy response.

Cancer cell-intrinsic MHC-II expression is associated with the Hippo signaling pathway

We then asked what regulates cancer cell-intrinsic MHC-II expression. Although multiple studies have explored the regulation of cancer cell-intrinsic MHC-II expression by *CIITA* (3,5,10), other genes regulating cancer cell-intrinsic MHC-II expression remain undetermined. To identify other potential regulators, we curated proteomic, transcriptomic, and epigenomic data from multiple collections of melanoma cell lines. Using mass spectrometry data from the CCLE, we examined the top genes associated with MHC-II protein abundance in melanoma (**Fig. 4A**). Major components of the MHC-II pathway, including *CD74*, *HLA-DR*, *HLA-DP*, and *HLA-DM* genes, were among the top associated genes. Other genes, including *NF2*, *PTPN14*, and *TAOK2*, were also among the top-ranked genes (**Fig. 4A**), and a common theme shared by these genes is that they participate in the Hippo signaling pathway. *NF2* is a well-established tumor suppressor, and loss of *NF2* increases the Hippo pathway activity (33-35). *PTPN14* is another established upstream regulator of the Hippo pathway and exerts its function through an interaction with *YAP1*, a major effector of the Hippo pathway. (36-38) Copy number loss for the TAOK family is also reported to be a major cause of elevated Hippo pathway activity (39).

The Hippo signaling pathway plays an important role in regulating tissue growth during development and regeneration. Upstream signals, including *NF2* and *AMOTL1/2,* activate downstream kinases such as large tumor suppressor 1/2 (LATS1 and LATS2*)*, which phosphorylate YAP/TAZ, major effectors of the Hippo signaling cascade, to prevent them from entering the nucleus (40-46). When in the nucleus, YAP/TAZ bind to transcription factors, such as the TEAD protein family, to promote the expression of genes related to cell proliferation and apoptosis (41-46). As the Hippo signaling pathway is heavily regulated by phosphorylation, we examined which phosphopeptides are most correlated with MHC-II by curating publicly available (phospho)proteome data from melanoma cells (19).The top positively/negatively correlated genes were enriched for the Hippo signaling pathway (**Fig. 4B-C**), suggesting that the phosphorylation of the Hippo signaling pathway is associated with MHC-II in melanoma cells.

RUNX1 is a member of the core-binding factor family of transcription factors. With its binding partner CBFB, RUNX1 transcriptionally inhibits YAP/TAZ expression (47-51). The interaction of RUNX1 with its co-factors is also among the top pathways enriched by MHC-II-correlated phosphoproteins (**Fig. 4C**). In addition to the proteomic analyses, we performed transcriptomic analyses to identify the gene expression programs associated with MHC-II expression in the cancer cells. Using the transcriptome profiles of 191 melanoma cell lines curated from 3 published studies (15,17,18), we evaluated the correlations between MHC-II mRNA and each gene's expression. *RUNX1* was also among the top associated genes with MHC-II expression in these studies (**Fig. 4D**). Together, these analyses suggest that RUNX1 and its binding partner CBFB might have the potential to inhibit YAP/TAZ resulting in enhanced cancer cell-intrinsic MHC-II expression.

Cancer cell-intrinsic MHC-II expression is regulated by the Hippo signaling pathway

Based on the correlations observed above, we sought to use orthogonal data to test the association between Hippo signaling pathway and MHC-II expression. Specifically, we curated ten melanoma cell lines where both transcriptome and open chromatin regions had been profiled (20). Consistent with the transcriptomic and proteomic data above, both transcription and chromatin accessibility of MHC-II were higher in cells with elevated chromatin accessibility of Hippo signaling pathway genes ($p < 0.001$) (**Fig. 5A**). This raised the possibility of Hippo signaling pathway regulation of MHC-II at the transcriptional level and prompted us to analyze published transcriptomic data on Hippo pathway perturbation. We curated a study that profiled gene expression in the MM047 melanoma line when all four TEADs (*TEAD1*, *TEAD2*, *TEAD3*, *TEAD4*) were simultaneously knocked down with siRNAs (**Fig. 5B**) (20). Indeed, the simultaneous KD of TEADs significantly increased the expression of MHC-II, supporting the Hippo-mediated regulation of MHC-II transcription (**Fig. 5C**). MHC-I mRNA abundance, however, remained the same after TEADs perturbation (**Fig. 5C**).

We further experimentally validated the effect of Hippo signaling pathway perturbation on MHC-II expression using CRISPR-mediated single-gene knockouts targeting *NF2*, *AMOTL1/2*, *LATS1/2*, *RUNX1*, and *CBFB* in the human melanoma cell line A375. *CIITA*, a master regulator of MHC-II, was also knocked out as a positive control (**Fig. 6A**). Consistent with our computational prediction, deletion of *NF2*, AMOTL2, *LATS2*, *RUNX1*, and *CBFB* significantly decreased MHC-II expression (**Fig. 6B**), confirming that MHC-II is regulated by the Hippo signaling pathway in melanoma cells. The Hippo signaling pathway is known to regulate multiple cellular processes, including cell proliferation, differentiation, and cell death, through inhibiting YAP/TAZ. Our study reveals a novel role of this pathway in cancer MHC-II expression (**Fig. 6C**).

Discussion

Multiple studies have identified cancer cell-intrinsic MHC-II expression and its association with better anti-tumor immune response (4,7,8). However, it is unclear how widely MHC-II is expressed in solid tumor cancer cells and whether the natural variation of MHC-II abundance in cancer cells has causal effects in the anti-tumor immune response. Moreover, it remains elusive how MHC-II expression is regulated in cancer cells. We attempted to address these questions by leveraging comprehensive data mining to predict the putative regulators and targeted experiments to validate our predictions.

We systematically characterized the cancer cell-intrinsic MHC-II expression landscape and found heterogeneous expression across cancer types, with the highest expression among solid tumors found in skin cancer. Comparison of the *in vivo* anti–PD-1 response of MHC-II-high and MHC-II-low isogenic cancer cells suggested that higher cancer cell-intrinsic MHC-II expression may potentiate immunotherapy. Computational analyses of publicly available multiomic data followed by experimental validation revealed the potential role of the Hippo signaling pathway in regulating cancer cell-intrinsic MHC-II expression in melanoma. The Hippo pathway is known to be a key regulator of tissue growth (40-42). Multiple studies have proposed inhibition of YAP/TAZ or TEAD as a cell-autonomous approach to suppress tumor growth (52-54). Other studies reported that upstream kinases of the Hippo pathway can suppress PD-L1 expression (55). In addition, our study suggests that modulating the Hippo signaling pathway might have an additional benefit for improving antigen presentation via upregulating MHC-II, thereby sensitizing cancer cells to anti-tumor immunity. These findings raise the possibility of improving immunotherapy response by modulating cancer cell-intrinsic MHC-II through activating the Hippo signaling pathway.

Our analyses of CCLE data suggest that skin cancer has the highest MHC-II expression, but MHC-II can also be expressed in other cancer types. For example, Oh et al. found that MHC-II-expressing bladder cancer cells can be killed by intratumoral CD4+ cytotoxic T cells (4). Johnson et al. and Eddine et al. found that enforced expression of CIITA can elevate MHC-II expression in cancer cells and sensitize them to CD4+ T cell–driven cytotoxicity (11,12). These studies comport with our finding that cancer cell-intrinsic MHC-II expression is a critical factor for anti-tumor immune response and suggest future endeavors toward targeting cancer cells through enhancing cancer cell-intrinsic MHC-II expression. Future studies are also needed to validate whether Hippo signaling pathway regulates MHC-II in other solid tumor cancer cells.

One caveat of our study is the low sensitivity of proteomic data we curated for association studies. 8,100 proteins were detected in mass-spectrometry data (19), which limits the power of identifying protein signaling events associated with MHC-II expression. In addition, phosphorylation of proteins may be poorly reflected in RNA-Seq data, limiting the ability to integrate proteomic and genomic data. Another caveat is the small sample size of several public studies, such as the phosphoproteome cohort (n=6). Nevertheless, we identified the Hippo pathway to be strongly correlated with MHC-II expression and validated its regulatory function. This does not exclude other regulators, which need to be systematically probed by future experiments such as CRISPR screens.

In summary, we integrated data mining and experimental validation to assess the function and regulation of cancer cell-intrinsic MHC-II expression. We revealed that high expression of MHC-II is associated with better immunotherapy responses, and MHC-II expression can be regulated by the Hippo signaling pathway in melanoma. Our findings raised the possibility of modulating the Hippo signaling pathway to enhance MHC-II expression and potentiate immunotherapy.

Future studies are needed to address the effects of modulating the Hippo signaling pathway on immunotherapy response *in vivo* and in the clinic.

Acknowledgements

We acknowledge authors from published studies for sharing their data. We also acknowledge The International Immuno-Oncology Network (II-ON) for sharing the CheckMate 064 (NCT01783938) data.

References

1. Forlani G, Shallak M, Celesti F, Accolla RS. Unveiling the Hidden Treasury: CIITA-Driven MHC Class II Expression in Tumor Cells to Dig up the Relevant Repertoire of Tumor Antigens for Optimal Stimulation of Tumor Specific CD4+ T Helper Cells. Cancers **2020**;12(11) doi 10.3390/cancers12113181.
2. Roche PA, Furuta K. The ins and outs of MHC class II-mediated antigen processing and presentation. Nat Rev Immunol **2015**;15(4):203-16 doi 10.1038/nri3818.
3. Axelrod ML, Cook RS, Johnson DB, Balko JM. Biological Consequences of MHC-II Expression by Tumor Cells in Cancer. Clin Cancer Res **2019**;25(8):2392-402 doi 10.1158/1078-0432.Ccr-18-3200.
4. Oh DY, Kwek SS, Raju SS, Li T, McCarthy E, Chow E*, et al.* Intratumoral CD4(+) T Cells Mediate Anti-tumor Cytotoxicity in Human Bladder Cancer. Cell **2020**;181(7):1612-25.e13 doi 10.1016/j.cell.2020.05.017.
5. Muhlethaler-Mottet A, Otten LA, Steimle V, Mach B. Expression of MHC class II molecules in different cellular and functional compartments is controlled by differential usage of multiple promoters of the transactivator CIITA. Embo j **1997**;16(10):2851-60 doi 10.1093/emboj/16.10.2851.
6. Lattime EC, Gomella LG, McCue PA. Murine bladder carcinoma cells present antigen to BCG-specific CD4+ T-cells. Cancer research **1992**;52(15):4286-90.
7. Johnson DB, Estrada MV, Salgado R, Sanchez V, Doxie DB, Opalenik SR*, et al.* Melanoma-specific MHC-II expression represents a tumour-autonomous phenotype and predicts response to anti-PD-1/PD-L1 therapy. Nature communications **2016**;7:10582 doi 10.1038/ncomms10582.
8. Rodig SJ, Gusenleitner D, Jackson DG, Gjini E, Giobbie-Hurder A, Jin C*, et al.* MHC proteins confer differential sensitivity to CTLA-4 and PD-1 blockade in untreated metastatic melanoma. Science translational medicine **2018**;10(450) doi 10.1126/scitranslmed.aar3342.

9. Roemer MGM, Redd RA, Cader FZ, Pak CJ, Abdelrahman S, Ouyang J*, et al.* Major Histocompatibility Complex Class II and Programmed Death Ligand 1 Expression Predict Outcome After Programmed Death 1 Blockade in Classic Hodgkin Lymphoma. Journal of clinical oncology : official journal of the American Society of Clinical Oncology **2018**;36(10):942-50 doi 10.1200/jco.2017.77.3994.
10. LeibundGut-Landmann S, Waldburger JM, Krawczyk M, Otten LA, Suter T, Fontana A*, et al.* Mini-review: Specificity and expression of CIITA, the master regulator of MHC class II genes. Eur J Immunol **2004**;34(6):1513-25 doi 10.1002/eji.200424964.
11. Johnson AM, Bullock BL, Neuwelt AJ, Poczobutt JM, Kaspar RE, Li HY*, et al.* Cancer Cell-Intrinsic Expression of MHC Class II Regulates the Immune Microenvironment and Response to Anti-PD-1 Therapy in Lung Adenocarcinoma. J Immunol **2020**;204(8):2295-307 doi 10.4049/jimmunol.1900778.
12. Bou Nasser Eddine F, Forlani G, Lombardo L, Tedeschi A, Tosi G, Accolla RS. CIITA-driven MHC class II expressing tumor cells can efficiently prime naive CD4(+) TH cells in vivo and vaccinate the host against parental MHC-II-negative tumor cells. Oncoimmunology **2017**;6(1):e1261777 doi 10.1080/2162402x.2016.1261777.
13. Eagle K, Harada T, Kalfon J, Perez MW, Heshmati Y, Ewers J*, et al.* Transcriptional Plasticity Drives Leukemia Immune Escape. Blood Cancer Discov **2022**;3(5):394-409 doi 10.1158/2643-3230.Bcd-21-0207.
14. Gambacorta V, Beretta S, Ciccimarra M, Zito L, Giannetti K, Andrisani A*, et al.* Integrated Multiomic Profiling Identifies the Epigenetic Regulator PRC2 as a Therapeutic Target to Counteract Leukemia Immune Escape and Relapse. Cancer Discov **2022**;12(6):1449-61 doi 10.1158/2159-8290.Cd-21-0980.
15. Ghandi M, Huang FW, Jane-Valbuena J, Kryukov GV, Lo CC, McDonald ER, 3rd*, et al.* Next-generation characterization of the Cancer Cell Line Encyclopedia. Nature **2019**;569(7757):503-8 doi 10.1038/s41586-019-1186-3.
16. Li B, Severson E, Pignon JC, Zhao H, Li T, Novak J*, et al.* Comprehensive analyses of tumor immunity: implications for cancer immunotherapy. Genome biology **2016**;17(1):174 doi 10.1186/s13059-016-1028-7.
17. Klijn C, Durinck S, Stawiski EW, Haverty PM, Jiang Z, Liu H*, et al.* A comprehensive transcriptional portrait of human cancer cell lines. Nature biotechnology **2015**;33(3):306-12 doi 10.1038/nbt.3080.
18. Paz H, Tsoi J, Kalbasi A, Grasso CS, McBride WH, Schaue D*, et al.* Interleukin 32 expression in human melanoma. Journal of translational medicine **2019**;17(1):113 doi 10.1186/s12967-019-1862-y.
19. Gao E, Li W, Wu C, Shao W, Di Y, Liu Y. Data-independent acquisition-based proteome and phosphoproteome profiling across six melanoma cell lines reveals determinants of proteotypes. Molecular omics **2021**;17(3):413-25 doi 10.1039/d0mo00188k.
20. Verfaillie A, Imrichova H, Atak ZK, Dewaele M, Rambow F, Hulselmans G*, et al.* Decoding the regulatory landscape of melanoma reveals TEADS as regulators of the invasive cell state. Nature communications **2015**;6:6683 doi 10.1038/ncomms7683.
21. Weber JS, Gibney G, Sullivan RJ, Sosman JA, Slingluff CL, Jr., Lawrence DP*, et al.* Sequential administration of nivolumab and ipilimumab with a planned switch in

patients with advanced melanoma (CheckMate 064): an open-label, randomised, phase 2 trial. Lancet Oncol **2016**;17(7):943-55 doi 10.1016/s1470-2045(16)30126-7.
22. Tirosh I, Izar B, Prakadan SM, Wadsworth MH, Treacy D, Trombetta JJ*, et al.* Dissecting the multicellular ecosystem of metastatic melanoma by single-cell RNA-seq. Science **2016**;352(6282):189-96.
23. Sanjana NE, Shalem O, Zhang F. Improved vectors and genome-wide libraries for CRISPR screening. Nature methods **2014**;11(8):783-4 doi 10.1038/nmeth.3047.
24. Sturm G, Finotello F, List M. Immunedeconv: An R Package for Unified Access to Computational Methods for Estimating Immune Cell Fractions from Bulk RNA-Sequencing Data. Methods in molecular biology (Clifton, NJ) **2020**;2120:223-32 doi 10.1007/978-1-0716-0327-7_16.
25. Li T, Fu J, Zeng Z, Cohen D, Li J, Chen Q*, et al.* TIMER2. 0 for analysis of tumor-infiltrating immune cells. Nucleic acids research **2020**;48(W1):W509-W14.
26. Aran D, Hu Z, Butte AJ. xCell: digitally portraying the tissue cellular heterogeneity landscape. Genome Biol **2017**;18(1):220 doi 10.1186/s13059-017-1349-1.
27. Newman AM, Liu CL, Green MR, Gentles AJ, Feng W, Xu Y*, et al.* Robust enumeration of cell subsets from tissue expression profiles. Nature methods **2015**;12(5):453-7 doi 10.1038/nmeth.3337.
28. Racle J, de Jonge K, Baumgaertner P, Speiser DE, Gfeller D. Simultaneous enumeration of cancer and immune cell types from bulk tumor gene expression data. Elife **2017**;6 doi 10.7554/eLife.26476.
29. Finotello F, Mayer C, Plattner C, Laschober G, Rieder D, Hackl H*, et al.* Molecular and pharmacological modulators of the tumor immune contexture revealed by deconvolution of RNA-seq data. Genome Med **2019**;11(1):34 doi 10.1186/s13073-019-0638-6.
30. Petitprez F, Levy S, Sun CM, Meylan M, Linhard C, Becht E*, et al.* The murine Microenvironment Cell Population counter method to estimate abundance of tissue-infiltrating immune and stromal cell populations in murine samples using gene expression. Genome medicine **2020**;12(1):86 doi 10.1186/s13073-020-00783-w.
31. Barbie DA, Tamayo P, Boehm JS, Kim SY, Moody SE, Dunn IF*, et al.* Systematic RNA interference reveals that oncogenic KRAS-driven cancers require TBK1. Nature **2009**;462(7269):108-12.
32. Squair JW, Gautier M, Kathe C, Anderson MA, James ND, Hutson TH*, et al.* Confronting false discoveries in single-cell differential expression. Nature communications **2021**;12(1):1-15.
33. Sourbier C, Liao P-J, Ricketts CJ, Wei D, Yang Y, Baranes SM*, et al.* Targeting loss of the Hippo signaling pathway in NF2-deficient papillary kidney cancers. Oncotarget **2018**;9(12):10723.
34. Hong AW, Meng Z, Plouffe SW, Lin Z, Zhang M, Guan K-L. Critical roles of phosphoinositides and NF2 in Hippo pathway regulation. Genes & development **2020**;34(7-8):511-25.
35. Wu J, Minikes AM, Gao M, Bian H, Li Y, Stockwell BR*, et al.* Intercellular interaction dictates cancer cell ferroptosis via NF2-YAP signalling. Nature **2019**;572(7769):402-6 doi 10.1038/s41586-019-1426-6.

36. Wilson KE, Yang N, Mussell AL, Zhang J. The Regulatory Role of KIBRA and PTPN14 in Hippo Signaling and Beyond. Genes (Basel) **2016**;7(6) doi 10.3390/genes7060023.
37. Liu X, Yang N, Figel SA, Wilson KE, Morrison CD, Gelman IH*, et al.* PTPN14 interacts with and negatively regulates the oncogenic function of YAP. Oncogene **2013**;32(10):1266-73 doi 10.1038/onc.2012.147.
38. Wang W, Huang J, Wang X, Yuan J, Li X, Feng L*, et al.* PTPN14 is required for the density-dependent control of YAP1. Genes Dev **2012**;26(17):1959-71 doi 10.1101/gad.192955.112.
39. Boggiano JC, Vanderzalm PJ, Fehon RG. Tao-1 phosphorylates Hippo/MST kinases to regulate the Hippo-Salvador-Warts tumor suppressor pathway. Developmental cell **2011**;21(5):888-95 doi 10.1016/j.devcel.2011.08.028.
40. Bao Y, Hata Y, Ikeda M, Withanage K. Mammalian Hippo pathway: from development to cancer and beyond. J Biochem **2011**;149(4):361-79 doi 10.1093/jb/mvr021.
41. Calses PC, Crawford JJ, Lill JR, Dey A. Hippo Pathway in Cancer: Aberrant Regulation and Therapeutic Opportunities. Trends Cancer **2019**;5(5):297-307 doi 10.1016/j.trecan.2019.04.001.
42. Dey A, Varelas X, Guan KL. Targeting the Hippo pathway in cancer, fibrosis, wound healing and regenerative medicine. Nat Rev Drug Discov **2020**;19(7):480-94 doi 10.1038/s41573-020-0070-z.
43. Harvey KF, Zhang X, Thomas DM. The Hippo pathway and human cancer. Nat Rev Cancer **2013**;13(4):246-57 doi 10.1038/nrc3458.
44. Zeng Q, Hong W. The emerging role of the hippo pathway in cell contact inhibition, organ size control, and cancer development in mammals. Cancer Cell **2008**;13(3):188-92 doi 10.1016/j.ccr.2008.02.011.
45. Gumbiner BM, Kim NG. The Hippo-YAP signaling pathway and contact inhibition of growth. J Cell Sci **2014**;127(Pt 4):709-17 doi 10.1242/jcs.140103.
46. Manmadhan S, Ehmer U. Hippo Signaling in the Liver - A Long and Ever-Expanding Story. Front Cell Dev Biol **2019**;7:33 doi 10.3389/fcell.2019.00033.
47. Kulkarni M, Tan TZ, Syed Sulaiman NB, Lamar JM, Bansal P, Cui J*, et al.* RUNX1 and RUNX3 protect against YAP-mediated EMT, stem-ness and shorter survival outcomes in breast cancer. Oncotarget **2018**;9(18):14175-92 doi 10.18632/oncotarget.24419.
48. Meng G, Wei J, Wang Y, Qu D, Zhang J. miR-21 regulates immunosuppression mediated by myeloid-derived suppressor cells by impairing RUNX1-YAP interaction in lung cancer. Cancer cell international **2020**;20:495 doi 10.1186/s12935-020-01555-7.
49. Okuda T, van Deursen J, Hiebert SW, Grosveld G, Downing JR. AML1, the target of multiple chromosomal translocations in human leukemia, is essential for normal fetal liver hematopoiesis. Cell **1996**;84(2):321-30 doi 10.1016/s0092-8674(00)80986-1.
50. Wang Q, Stacy T, Binder M, Marin-Padilla M, Sharpe AH, Speck NA. Disruption of the Cbfa2 gene causes necrosis and hemorrhaging in the central nervous system and blocks definitive hematopoiesis. Proceedings of the National Academy of Sciences of the United States of America **1996**;93(8):3444-9 doi 10.1073/pnas.93.8.3444.
51. Pan Z, Tian Y, Cao C, Niu G. The Emerging Role of YAP/TAZ in Tumor Immunity. Molecular cancer research : MCR **2019**;17(9):1777-86 doi 10.1158/1541-7786.Mcr-19-0375.

52. Liu-Chittenden Y, Huang B, Shim JS, Chen Q, Lee S-J, Anders RA*, et al.* Genetic and pharmacological disruption of the TEAD–YAP complex suppresses the oncogenic activity of YAP. Genes & development **2012**;26(12):1300-5.
53. Chang L, Azzolin L, Di Biagio D, Zanconato F, Battilana G, Xiccato RL*, et al.* The SWI/SNF complex is a mechanoregulated inhibitor of YAP and TAZ. Nature **2018**;563(7730):265-9.
54. Dominguez-Berrocal L, Cirri E, Zhang X, Andrini L, Marin GH, Lebel-Binay S*, et al.* New therapeutic approach for targeting hippo signalling pathway. Scientific reports **2019**;9(1):1-11.
55. Janse van Rensburg HJ, Azad T, Ling M, Hao Y, Snetsinger B, Khanal P*, et al.* The Hippo Pathway Component TAZ Promotes Immune Evasion in Human Cancer through PD-L1. Cancer research **2018**;78(6):1457-70 doi 10.1158/0008-5472.Can-17-3139.

Tables and Figure legends

Table 1. Multiomics data derived from large collections of cancer cells and patient samples.

Knockdown (KD); immunohistochemistry (IHC); *TEAD1*, *TEAD2*, *TEAD3*, *TEAD4* (TEADs)

	Source	**Data type**	**Sample size**	**Description**
CCLE	DepMap(15)	RNA-Seq	1362	human cancer cell line
Klijina et al.(17)	ArrayExpress: E-MTAB-2706	RNA-Seq	675	human cancer cell line
Tosi et al.(18)	GEO: GSE80829	RNA-Seq	54	melanoma cell line
Verfaillie et al. (20)	GEO: GSE60666	RNA-Seq; FAIRE-Seq	10	melanoma cell line
Gao et al.(19)	GEO: GSE162270	Mass Spec (phospho)proteome	6	melanoma cell line
CCLE	DepMap(15)	Mass Spec proteome	367	human cancer cell line
Verfaillie et al. (20)	GEO: GSE60666	RNA-Seq after TEADs KD	6	melanoma cell line
Weber et al. (21) Rodig et al. (8)	BMS (NCT01783938)(21) Rodig et al. (8)	RNA-seq; IHC of cancer cell specific MHC-I and MHC-II	93	melanoma samples from human clinical trial
Tirosh et al. (22)	GEO: GSE72056	scRNA-Seq	4645 cells from 19 patients	melanoma samples

639 **Table 2**. gRNA sequences for different genes.

Gene	gRNA sequences
CIITA	ACACTCACTCCATCACCCGG, CCACATGAGGACACCTCCGA, CAGCAGCAAGAGCCTGGAG, CCAGTACATGTGCATCAGG
NF2	CTTGGTACGCAGAGCACCG, GAGATGGAGTTCAATTGCG, ACCCCAGTGTTCACAAGCG, GAGGAGGCTGAACGCACGA
AMOTL1	CAGCCTCAGCAGAACAACG, ATGGTGGAGATATTAACAG, ATGAATAAACCTGCCTCGG, CTCGTTACCCCATACTCAG
AMOTL2	CGGCGCCATCGAGGACCAG, GCCCACTCGCAGTACTATG, ATGAGCTAGTACAACATGA, AGGCTGCAAGACTTCAACC
LATS1	CAGCCATCTGCTCTCGTCG, TAACACTCCTTACTTGAGG, TTGATTAGGAGGATTCATG, CTTCTGCTTTACAAACAGG
LATS2	CCAGCAGAAGGTTAACCGG, TAGGACGCAAACGAATCGC, GAGCCGCAAAAGCGCCAAG, TTGCTGATGTACTCCAGGG
RUNX1	GCAGTGGAGTGGTTCAGGG, ACTTCGACCGACAAACCTG, TGATCGTAGGACCACGGTG, AGATGATCAGACCAAGCCC
CBFB	GAGTCTGTGTTATCTGGAA, AGTCGACATACTCTCGGCT, CTGCCTCACCTCACACTCG, CCGACTTACGATTTCCGAG

640

641 **Figure Legends**

642 **Fig. 1 High cancer cell-intrinsic MHC-II is associated with favorable immunotherapy**
643 **outcomes (A)** Quantification of cancer cell-intrinsic MHC-II protein in each of the immune-
644 checkpoint blockade (ICB) response group or progression free survival (PFS) group. Box plots
645 represent the quartiles of protein abundance. **(B)** Kaplan–Meier overall survival curves for
646 cancer cell-intrinsic MHC-II-high and -low groups. The cohorts were split into high and low
647 groups using a cutoff of MHC-II >1%. **(C-D)** Rank plot of the correlation coefficients for all
648 inferred immune cell infiltrates and the associated cancer cell-intrinsic MHC-I (**C**) and MHC-II (**D**)
649 protein. Cancer cell-intrinsic MHC protein was quantified by immunohistochemistry (IHC).
650 [Please include the statistical test used to calculate p-val in 1A]

Fig. 2 MHC-II is highly expressed in skin cancer cell lines. (A) MHC-II mRNA in a diverse panel of 1,362 human cancer cell lines from the Cancer Cell Line Encyclopedia (CCLE). Cancer cell lines were grouped by cancer type. **(B)** MHC-II mRNA in a diverse panel of 675 human cancer cell lines from the Klijina study. **(C)** The correlation between MHC-II mRNA and protein in skin cancer cell lines. The protein was quantified by mass spectrometry. [Please include the statistical test used to calculate p-val in 2C]

Fig. 3 Cancer cell-intrinsic MHC-II expression affects immunotherapy response. (A) Illustration of the *in vivo* experiment design. Longitudinal tumor size of MHC-II-high or -low B16F10 tumors treated with control IgG or anti–PD-1 (2 sites/mouse, 10 mice/group). $4x10^5$ B16F10 cells (MHC-II-high or -low sorted cells) were transplanted subcutaneously into syngeneic recipient mice. From day 3 post-transplantation, recipient mice were treated with control IgG or anti–PD-1 every 3rd day for a total of 4 doses. **(B)** Tumor size and recipient survival was monitored. Mean ± SEM is shown for each group at each time point. (**P < 0.01, ***P < 0.001; Two-way ANOVA with Benjamini-Hochberg post-*hoc* test).

Fig. 4 Cancer cell-intrinsic MHC-II expression is associated with the Hippo signaling pathway. (A) Volcano plot of all genes associated with MHC-II protein abundance in melanoma cell lines. Statistical significance (log_{10}adjusted p-value) was plotted against correlation coefficients between gene and MHC-II protein abundance. **(B)** Rank plot of the correlation coefficients for all phosphopeptides associated with MHC-II protein abundance. Phosphopeptides and protein abundance were measured by mass spectrometry. **(C)** Gene set enrichment using the significant genes from (B). **(D)** Venn diagram of genes significantly associated with MHC-II mRNA in melanoma cell lines from the CCLE (n=83), Klijina (n=54), and Tsoi (n=53) studies.

Fig. 5 Cancer cell-intrinsic MHC-II expression is affected by the Hippo signaling pathway. **(A)** Histogram, density plot, and heatmap of transcription and chromatin accessibility of MHC-II and Hippo signaling pathway genes. Read density across transcription start sites (TSS) within 2kb of *HLA-DRA* gene and hippo signaling pathway genes were evaluated. **(B)** Quantification of TEADs mRNA in control and TEADs knocked down groups. *TEAD1*, *TEAD2*, *TEAD3*, *TEAD4* were knocked down simultaneously with siRNAs. **(C)** Quantification of MHC-I and MHC-II mRNA in control and TEADs knocked down groups. [Please include the statistical test used to calculate p-val in 5B-C]

Fig. 6 Cancer cell-intrinsic MHC-II expression is regulated by the Hippo signaling pathway. (A) Representative plots of *HLA-DR* from flow cytometry. A375 cells were transduced with a plasmid encoding Cas9 and sgRNA targeting the control *AAVS1* region or *CIITA* followed by MHC-II quantification. The “Neg” group represents A375 cells incubated without anti-HLA-DR. **(B)** Validation of potential MHC-II regulators (4 sgRNAs per gene during virus production). **(C*)*** Illustration of the Hippo signaling pathway in regulating MHC-II in melanoma cells.

Figure 1

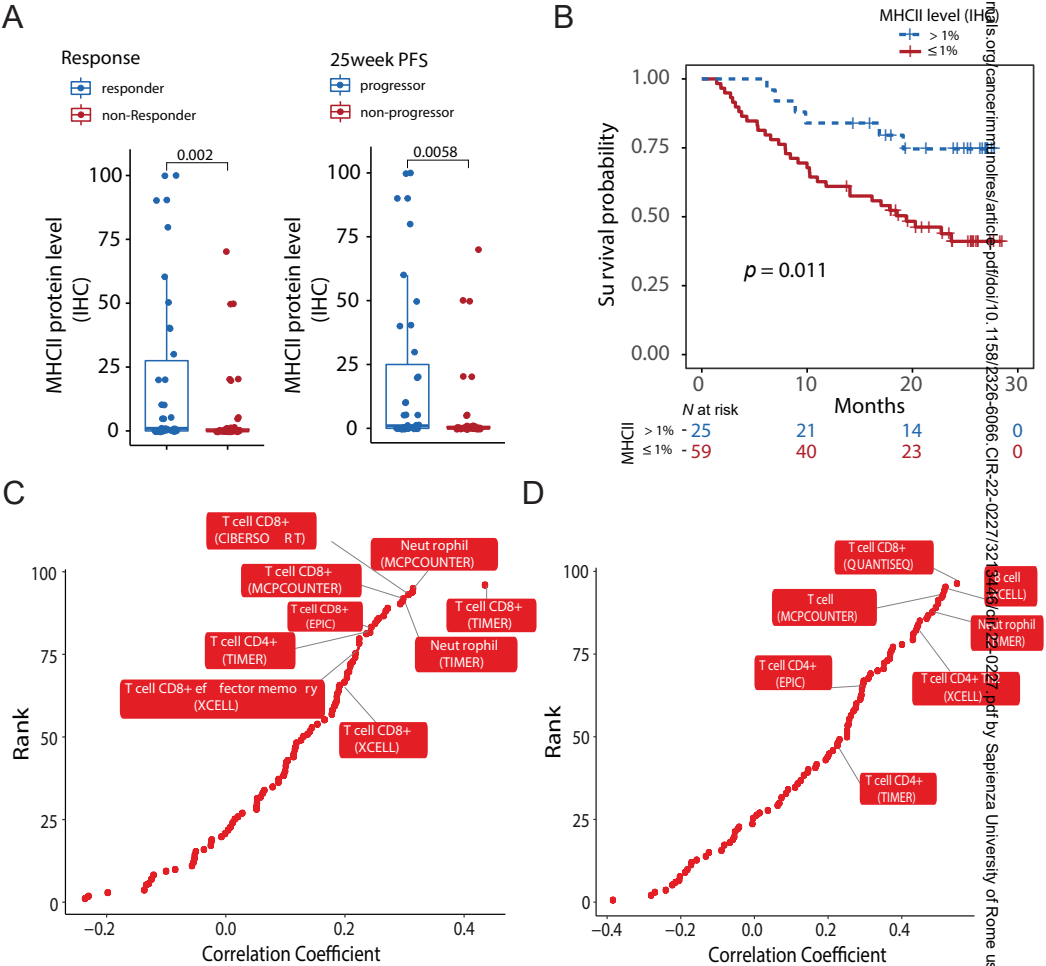

Figure 2

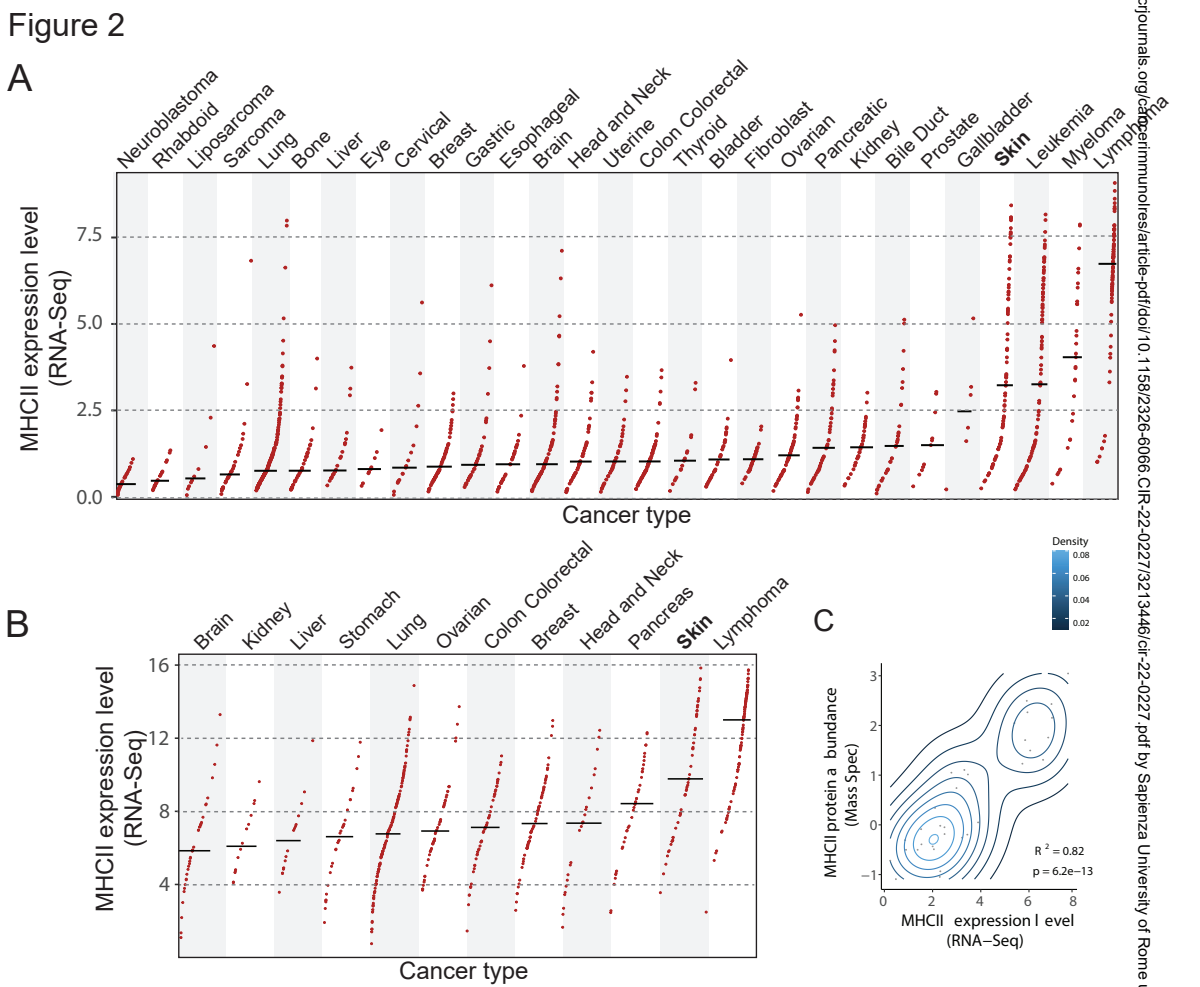

Figure 3

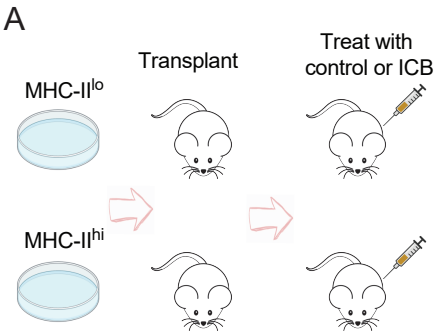

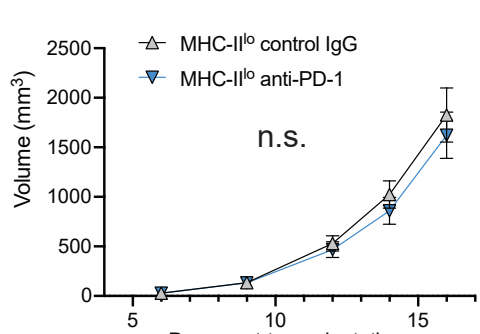

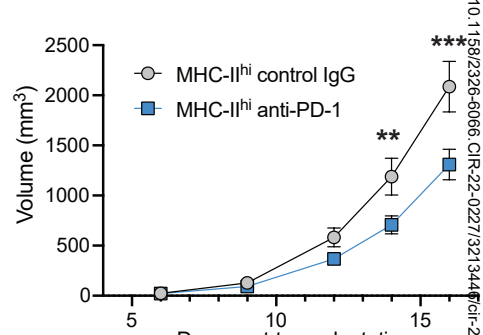

Figure 4

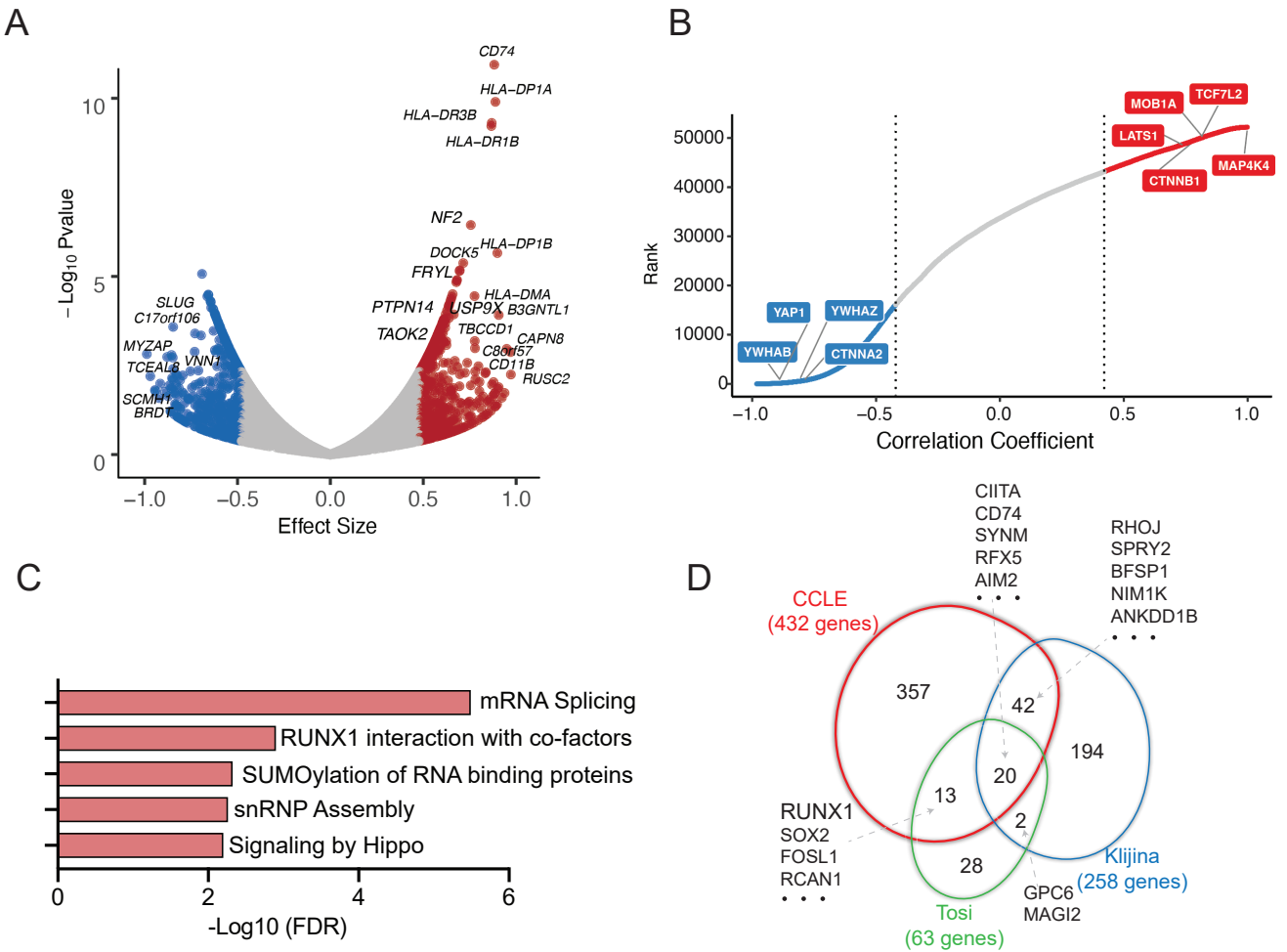

Figure 5

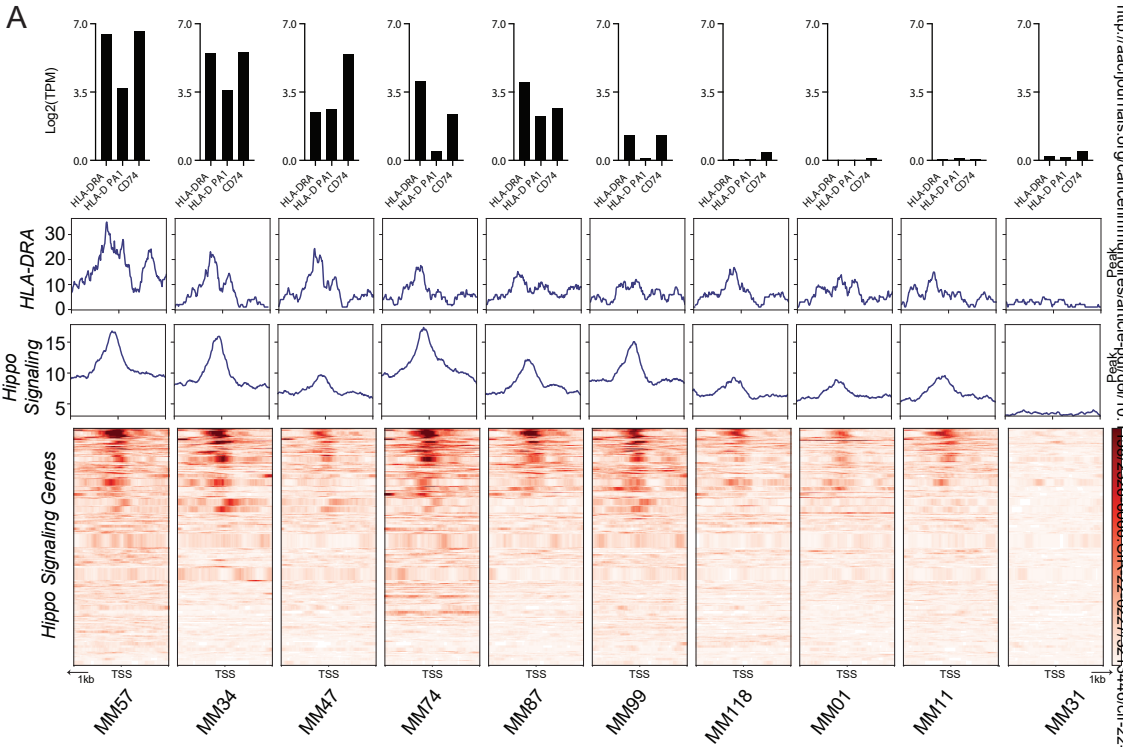

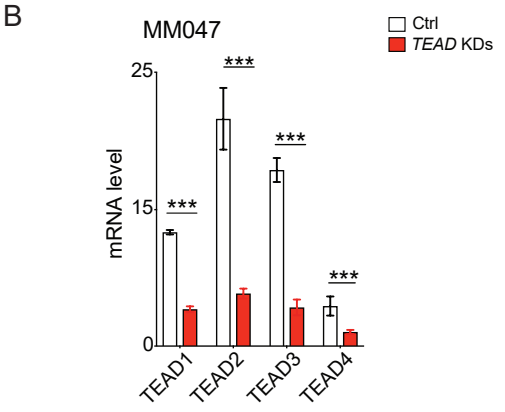

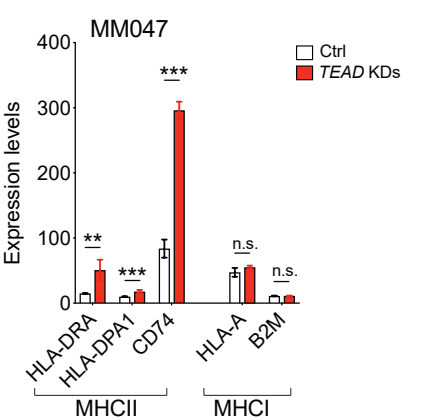

Figure 6